

Low-friction flows of liquid at nanopatterned interfaces

CÉCILE COTTIN-BIZONNE, JEAN-LOUIS BARRAT*, LYDÉRIC BOCQUET AND ELISABETH CHARLAIX

Laboratoire de Physique de la Matière Condensée et Nanostructures, CNRS and Université de Lyon, Bâtiment Léon Brillouin, 43 Boulevard du 11 Novembre, 69622 Villeurbanne Cedex, France

*e-mail: barrat@ipm.cn.univ-lyon1.fr

Published online: 9 March 2003; doi:10.1038/nmat857

With the important development of microfluidic systems, miniaturization of flow devices has become a real challenge. Microchannels, however, are characterized by a large surface-to-volume ratio, so that surface properties strongly affect flow resistance in submicrometre devices. We present here results showing that the concerted effect of wetting properties and surface roughness may considerably reduce friction of the fluid past the boundaries. The slippage of the fluid at the channel boundaries is shown to be greatly increased by using surfaces that are patterned on the nanometre scale. This effect occurs in the regime where the surface pattern is partially dewetted, in the spirit of the 'superhydrophobic' effects that have been discovered at macroscopic scales¹. Our results show for the first time that, in contrast to common belief, surface friction may be reduced by surface roughness. They also open the possibility of a controlled realization of the 'nanobubbles'² that have long been suspected to play a role in interfacial slippage^{3,4}.

The nature of the boundary condition for fluid flows past solid surfaces has long been a subject of interest^{5,6}, which has been revived by a large number of experiments and new theoretical approaches. The possibility of investigating flows at small scales in a quantitative manner, as opened by the development of nanoscale measurements (surface force apparatus or atomic force microscope), has allowed a number of experimental determinations of the 'slip length' δ (see Fig. 1) that is used to characterize this boundary condition^{7–12}. Optical techniques, such as fluorescence correlation or recovery methods^{13,14}, have also shown evidence for the existence of a non-zero slip length.

From a theoretical point of view, the parameters controlling the magnitude of the slip length are still largely unknown. At a macroscopic scale, the strength of the interaction between a solid and a liquid is most obviously characterized through the wetting behaviour. Weak interactions result in non-wetting behaviour, with large contact angles for a drop of liquid resting on the solid substrate. This characterization is purely thermodynamic, and has in principle no direct influence on the nature of fluid flow past the interface. Molecular dynamics studies and mode-coupling calculations^{15–17}, however, have shown that wettability of a perfect surface can be correlated to the magnitude of the hydrodynamic slippage. Qualitatively, a non-wettable substrate is only weakly coupled to the liquid, with a depleted surface layer that can be seen as an atomic-scale 'air cushion'. Therefore momentum transfer

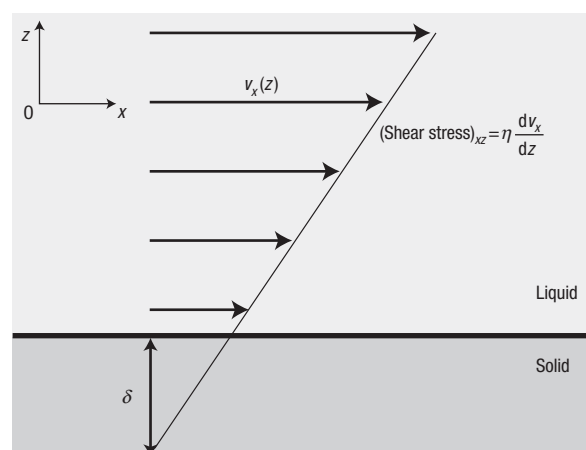


Figure 1 Definition of the slip length. The linear velocity (v_x) profile in the flowing, newtonian fluid (characterized by a newtonian viscosity η and a constant shear stress) does not vanish at the solid boundary. Extrapolation into the solid at a depth δ is necessary to obtain a vanishing velocity, as assumed by the macroscopic 'no-slip' boundary condition.

parallel to the interface is inefficient, and a large 'slip length' results.

Experimentally, it appears that although wettability is an important parameter, different results can be obtained for substrate/liquid combinations with similar wetting properties^{11–13,18}. Another parameter of obvious importance, which may explain such variability, and has not been taken into account previously in molecular simulations, is surface roughness. In fact, it has been shown¹⁹ that roughness suppresses slippage on a macroscopic scale, for any type of microscopic conditions.

Experiments¹¹ have indeed shown that, in a situation where slippage is observed on smooth surfaces, it can be suppressed by increasing surface roughness. Other experiments²⁰ on highly water-repellent walls (walls that had a pattern of narrow parallel grooves) resulted in important slippage at the wall. In this work, we present a numerical study of slippage at interfaces bearing a model roughness, which takes

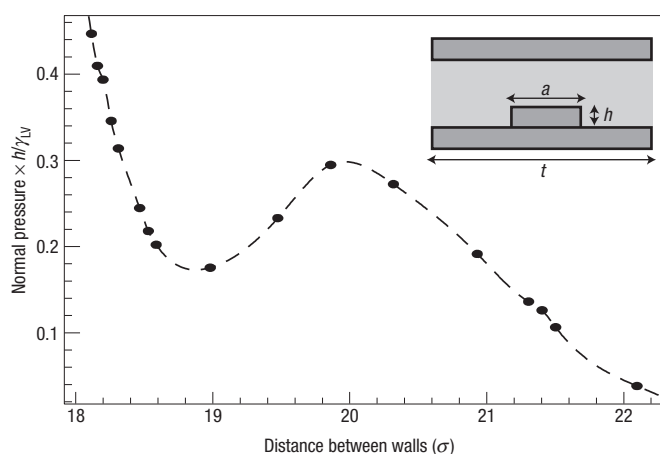


Figure 2 Normal pressure versus the distance between the walls. To facilitate comparison with experimental situations, the pressure has been rescaled by the typical pressure $\gamma_{LV}h$ (typically 100 bars for dots of 7 nm in water). The dashed line is a guide to the eye. The inset is used to define the main geometrical variables that describe our set-up. The curve shown in the figure corresponds to $h = 5\sigma$, $t = 20\sigma$, $a = 6.6\sigma$. With these parameters, a direct application of the macroscopic equation (3), with $\cos\theta = -0.74$ (ref. 16), would yield a coexistence pressure $P_{\text{coex}}h/\gamma_{LV} = 0.014$. Note that the range of distances for which the pressure increases with h is thermodynamically unstable, its observation being an artefact of small size simulations, corresponding to a ‘van der Waals loop’.

the form of a nanoscale periodic pattern. The effect of such patterns on wetting properties has been studied extensively, both experimentally and theoretically, but their influence on dynamics has received much less attention.

The configuration considered in our study is a fluid film confined between two parallel solid walls. The bottom wall is decorated with a periodic array of square-shaped dots of height h and width a (see Fig. 2). The typical lateral size of the cell is $L_x = L_y = t = 20\sigma$, where σ is the molecular diameter. Periodic boundary conditions in the directions x and y parallel to the wall are used. In our simulations, all the interactions are of the Lennard–Jones type

$$v_{ij}(r) = 4\epsilon[(\sigma/r)^{12} - c_{ij}(\sigma/r)^6] \quad (1)$$

The atoms in the fluid and the solid have the same molecular diameter, σ and interaction energies, ϵ ; r is the distance between two atoms. The parameter c_{ij} (the index $i, j = F, S$ refers to the fluid or solid phase) is a convenient control that can be varied to adjust the surface tension. The solid substrate is described by atoms fixed on the (100) plane of a face-centred-cubic lattice. We have worked with two values of c_{FS} , 0.5 and 0.8, which correspond to contact angles (deduced from Young’s law) of $\theta = 137^\circ$ or $\theta = 110^\circ$, respectively¹⁷. The simulations were carried out at constant temperature $k_B T/\epsilon = 1$, where k_B is Boltzmann’s constant, and T is temperature. In flow experiments, the velocity component in the directions orthogonal to the flow was thermostatted¹⁷ to avoid viscous heating within the fluid film. All results reported are obtained within a linear-response regime. Most numerical results are given here in Lennard–Jones units (L.J.u.).

We first briefly describe the static properties of the system, which were obtained using the following procedure. For a fixed number of liquid atoms, N_L , and distance between the walls, the normal pressure is obtained from the average force on the substrates along the z direction. This normal pressure can be varied either by changing the distance between the two walls at a fixed surface density, or by modifying the number of particles at fixed distance.

Figure 2 shows the pressure curve obtained when changing the distance between the walls. Two branches separated by a typical ‘van der Waals loop’ are clearly visible, indicating the existence of a phase transition between two possible situations. At higher normal pressures, the liquid occupies the full width of the cell, including the grooves separating the square dots. At lower pressures, partial dewetting is observed and a composite interface is formed, the space between the dots being essentially free from liquid atoms (see Fig. 3). Note that the range of pressure in Fig. 2 is rather small, so that the properties of the bulk fluid over this range are essentially constant (the relative density change being typically less than 0.2%)

In spite of the very small sizes involved, a qualitative interpretation of the observed behaviour can easily be given in terms of macroscopic capillarity. If we consider a system at fixed normal pressure P_N , the difference in Gibbs free energies between the wetted configuration (case A) and the formation of a composite interface (case B) can be written as:

$$G_B - G_A = (t^2 + 4ah - a^2)(\gamma_{LV}\cos\theta) + (t^2 - a^2)\gamma_{LV} + P_N(t^2 - a^2)h, \quad (2)$$

where γ_{LV} is the liquid–vapour surface tension and h the height of the dot. The composite interface is therefore favoured when

$$P_N < P_{\text{composite}} = -\gamma_{LV}(\cos\theta + 1)/h - 4a\gamma_{LV}\cos\theta/(t^2 - a^2). \quad (3)$$

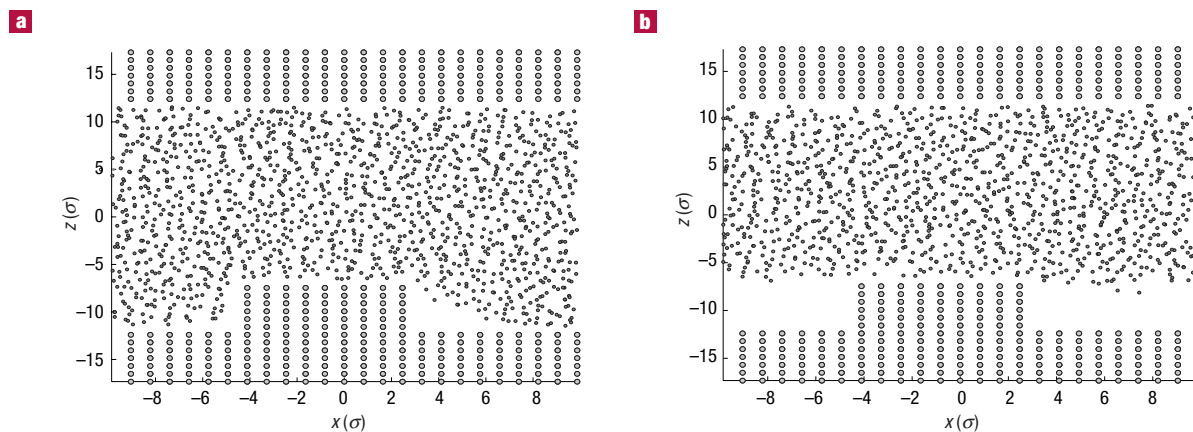


Figure 3 Flow patterns under different conditions. **a**, Transverse view of the atomic configuration in the wetted situation. Atoms belonging to the liquid and solid are represented by points and round dots, respectively. The liquid occupies nearly all the available volume. **b**, A composite interface is formed under low-pressure.

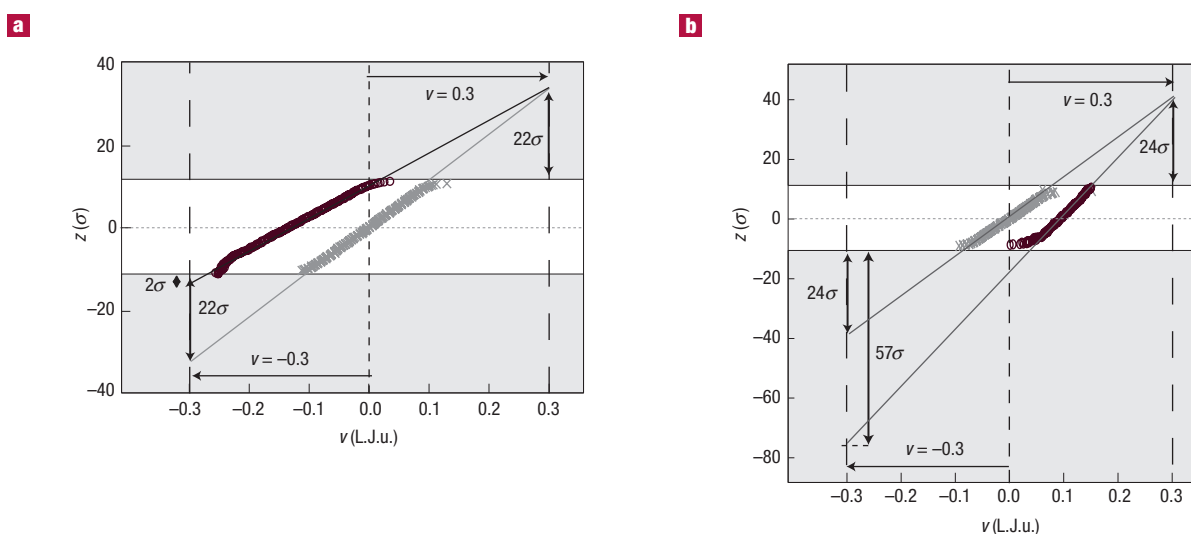


Figure 4 Velocity profiles for different conditions. **a**, Flow properties at a sheared solid–liquid interface, in a wetted situation. The normal pressure is $P = 0.086$ L.J.u. Black circles: Velocity profile in the presence of a square pattern on the bottom wall. Grey crosses: Velocity profile with two smooth walls (at the pressure $P = 0.086$ L.J.u.). The walls were moved at fixed velocities $U = \pm 0.3$ L.J.u. Slip lengths (arrows) are deduced from the intersections of the velocity profiles with the axis $v = \pm 0.3$. Numerically, $\delta = 22\sigma$ at the flat wall and $\delta = 2\sigma$ at the patterned wall. **b**, As for **a** but for a composite interface. The normal pressure is $P = 0.024$ L.J.u. One now finds, $\delta = 24\sigma$ at the flat wall and $\delta = 57\sigma$ at the patterned wall.

Although a quantitative agreement can hardly be expected in view of the small sizes in our system, we have checked that equation (3) correctly predicts the general trends observed in our simulation, when the height or width or the square dots are varied. It can be used, for example, to understand the influence of an increase in the corrugation wavelength (t and a). At fixed h , such an increase results in a decrease of $P_{\text{composite}}$ down to unreachable negative pressures. However, dewetting may persist up to large, say micrometre, scales for appropriately chosen asperity sizes¹.

We now consider the essential objective of our study, namely the influence of roughness on dynamic properties of the confined fluid layers. Our study involved parallel Couette flow, in which the upper wall is moved with velocity U and the lower wall is moved with a velocity $-U$ (typically $U = 0.3$ in reduced L.J.u.). The temperature is kept constant by thermostatting through velocity rescaling in the direction perpendicular to the flow. For flat walls¹⁶, the slip length δ is defined as the distance between the wall position and the depth at which the extrapolated velocity profile, v , reaches the nominal wall velocity (that is, $v = U$). In the presence of square dots, the same definition is used. Obviously the presence of dots makes the choice of the wall position somewhat arbitrary. We choose to define the wall as the position of the bottom layer of substrate.

In the following, we will discuss the particular case of a fluid–solid interaction $c_{\text{FS}} = 0.5$, which corresponds to a contact angle $\theta = 137^\circ$ on a flat substrate. For this particular value of the interaction, and in the range of pressures we have investigated, the fluid displays a moderate amount of slip at a flat interface, which can be characterized by a slip length δ in the range 20–25 σ (the actual value being slightly pressure dependent). Taking σ to be 0.5 to 1 nm, this corresponds to a value of 10–25 nm.

In the presence of the square dot pattern, two very different situations have to be distinguished. The first case is that of a completely wetted substrate (Fig. 3a). A typical velocity profile for this situation is shown in Fig. 4a. First, it is seen from this profile that the introduction of the patterned substrate does not modify the flow in the vicinity of the upper, structureless wall. This boundary can still be characterized by a slip length $\delta = 22\sigma$, identical to what would be obtained with two flat substrates at the same pressure. In contrast, the slip is strongly

suppressed at the lower wall, where it can be characterized by a value $\delta = 2\sigma$. This value would be slightly higher (7σ) if the corrugation was taken at the crest of the pattern, but would still be much smaller than the value obtained for a perfectly flat surface.

A completely different result is obtained in the case where the pressure is low enough such that a composite interface is formed (Fig. 3b). A typical velocity profile corresponding to this situation is shown in Fig. 4b. As in the wetted situation, the pattern on the lower wall does not modify the slip effect on the upper one. The slip effect on the lower wall is, on the other hand, strongly enhanced by the presence of the composite interface. Numerically, δ increases by a factor of about 2.5, reaching a value 57 σ .

Qualitatively, the increase in δ should be associated with the absence of friction at the vapour–liquid interface, which can be described by a zero-stress boundary condition¹⁸. Hence, increasing the liquid–vapour interfacial area by using a more ‘spiky’ pattern should result in larger δ . Using a smaller dot width ($a = 4.9\sigma$) we found indeed that δ could reach a value 130 σ . It is also interesting to compare these simulation results with what could be inferred from approximate hydrodynamic calculations such as those of Hocking²⁰. Hocking considered, in particular, flow past a composite interface, and showed that this results in a partial slip condition when the fluid filling the corrugation (in our case vapour) is of lower viscosity. Unfortunately, a direct comparison with our results is not possible, due to the use of rather different corrugation models and to the ‘no-slip’ condition used by Hocking at the molecular level. We nevertheless expect that our results should stimulate further work using continuum approaches.

Our results confirm that mesoscopic roughness at the solid–liquid interface can greatly modify the interfacial flow properties, in the same manner the static wetting properties are affected. Experimentally, very few results involving surfaces of controlled roughness are available, and, as mentioned above, these experiments yield contrasting results. We believe this variability may find its roots in different wetting situations realized at the mesoscale (from the nano to micrometre scale). It has also been advocated that the existence of ‘nanobubbles’ at the liquid–solid interface is an important factor in slippage phenomena. Our simulations, although they also do not, strictly

speaking, confirm the existence of such bubbles, show nevertheless that a composite interface can indeed enhance slippage considerably. In our simulations, this enhancement corresponds to an equilibrium situation that is rapidly achieved at such small scales. Regarding this point, the situation in experiments, often done with surfaces bearing a micrometre pattern, is less clear-cut because metastable trapping of bubbles (possibly of dissolved gases) may occur in submicrometre channels. However, the essential ingredient of the effect studied here, that is, dewetting, is known to be present on patterned surfaces, from the nanometre up to the micrometre scale. Therefore, although our simulations are performed at nanometre scales, a friction reduction is expected over a large range of length scale, up to microscale patterns. The effect is however expected to be stronger for the more spiky nanometre pattern. In fact, very spectacular decreases in the flow resistance of droplets have been reported²² on surfaces that were decorated with a spiky nanoscale pattern, whereas the effect of a similar microscale pattern was less pronounced.

In summary, use of patterned surfaces, treated to produce a 'water repellent' effect, appears to be a promising way towards devices that would allow the flow of liquids in small channels with very low flow resistance.

Received 20 November 2002; accepted 12 February 2003; published 9 March 2003.

References

1. Quéré, D. Fakir droplets. *Nature Mater.* **1**, 14–15 (2002).
2. Tyrell, J. W. G. & Attard, P. Images of nanobubbles on hydrophobic surfaces and their interactions. *Phys. Rev. Lett.* **87**, 176104 (2001).
3. Vinogradova, O. L. *et al.* Submicrocavity structure of water between hydrophobic and hydrophilic walls as revealed by optical cavitation. *J. Colloid Interface Sci.* **173**, 443–447 (1995).
4. de Gennes, P. G. On fluid/wall slippage. *Langmuir* **18**, 3413–3414 (2002).
5. Schnell, E. Slippage of water over nonwettable surfaces. *J. Appl. Phys.* **27**, 1149–1152 (1956).
6. Churaev, N. V., Sobolev, V. D. & Somov, A. N. Slippage of liquids over lyophobic solid-surfaces. *J. Colloid Interface Sci.* **97**, 574–581 (1984).
7. Chan, D. C. Y. & Horn, R. G. The drainage of thin liquid-films between solid-surfaces. *J. Chem. Phys.* **83**, 5311–5324 (1985).
8. Georges, J.-M., Millot, S., Loubet, J.-L. & Tonck, A. Drainage of thin liquid-films between relatively smooth surfaces. *J. Chem. Phys.* **98**, 7345–7360 (1993).
9. Baudry, J., Charlaix, E., Tonck, A. & Mazuyer, D. Experimental evidence for a large slip effect at a nonwetting fluid-solid interface. *Langmuir* **17**, 5232–5236 (2001).
10. Craig, V. S. J., Neto, C. & Williams, D. R. M. Shear-dependent boundary slip in an aqueous Newtonian liquid. *Phys. Rev. Lett.* **87**, 054504 (2001).
11. Zhu, Y. X. & Granick, S. Limits of the hydrodynamic no-slip boundary condition. *Phys. Rev. Lett.* **88**, 106102 (2002).
12. Cottin-Bizonne, C. *et al.* An experimental study of slipping length. *Eur. Phys. J. E* **9**, 47–53 (2002).
13. Pit, R., Hervet, H. & Léger, L. Direct experimental evidence of slip in hexadecane: Solid interfaces. *Phys. Rev. Lett.* **85**, 980–983 (2000).
14. Trethewey, D. C. & Meinhart, C. D. Apparent fluid slip at hydrophobic microchannels walls. *Phys. Fluids* **14**, L9–L12, (2002).
15. Thompson, P. A. & Robbins, M. O. Shear flow near solids – Epitaxial order and flow boundary conditions. *Phys. Rev. A* **41**, 6830–6837 (1990).
16. Barrat, J.-L. & Bocquet, L. Large slip effect at a nonwetting fluid-solid interface. *Phys. Rev. Lett.* **82**, 4671–4674 (1999).
17. Barrat, J.-L. & Bocquet, L. Influence of wetting properties on the hydrodynamic boundary condition at a fluid-solid interface. *Faraday Discuss.* **112**, 121–129 (1999).
18. Lauga, E. & Stone H. A. Effective pressure-driven Stokes flow. *J. Fluid Mech.* (in the press).
19. Richardson, S. No slip boundary condition. *J. Fluid Mech.* **59**, 707–719 (1973).
20. Watanabe, K., Udagawa, Y. & Udagawa, H. Drag reduction of Newtonian fluid in a circular pipe with a highly water-repellent wall. *J. Fluid Mech.* **381**, 225–238 (1999).
21. Hocking, L. M. A moving fluid interface on a rough surface. *J. Fluid Mech.* **76**, 801–817 (1976).
22. Kim, J. & Kim, C. J. Nanostructured surfaces for dramatic reduction of flow resistance in droplet based microfluidics. *Proc. 2002 IEEE Conf. MEMS, Las Vegas, Nevada* (in the press).

Acknowledgements

It is a pleasure to thank H.A. Stone for interesting discussions. We thank the DGA for its financial support, and the PSMN (ENS-Lyon) and CDCSP (University of Lyon) for the use of their computational facilities.

Correspondence and requests for materials should be addressed to J.-L.B.

Competing financial interests

The authors declare that they have no competing financial interests.